DMD Fast Forward. Published on December 29, 2011 as doi:10.1124/dmd.111.043067
This article has not been copyedited and formatted. The final version may differ from this version.

Species Differences in Tissue Distribution and Enzyme Activities of Arylacetamide Deacetylase in Human, Rat, and Mouse

Yuki Kobayashi, Tatsuki Fukami, Akinori Nakajima, Akinobu Watanabe, Miki Nakajima, and Tsuyoshi Yokoi

Drug Metabolism and Toxicology, Faculty of Pharmaceutical Sciences, Kanazawa University, Kakuma-machi, Kanazawa 920-1192, Japan

Running title: Species differences of AADAC

To whom all correspondence should be sent:

Tsuyoshi Yokoi, Ph.D.

Drug Metabolism and Toxicology

Faculty of Pharmaceutical Sciences

Kanazawa University

Kakuma-machi

Kanazawa 920-1192, Japan

Tel / Fax: +81-76-234-4407

E-mail: tyokoi@kenroku.kanazawa-u.ac.jp

Number of text pages: 22

Number of tables: 4

Number of figures: 6

Number of references: 29

Number of words in abstract: 246 words

Number of words in introduction: 627 words

Number of words in discussion: 1,560 words

Abbreviations: AADAC, arylacetamide deacetylase; CES, carboxylesterase; CYP, Cytochrome P450; FLU-1, 4-nitro-3-(trifluoromethyl)phenylamine; His, histidine; HJM, human jejunum microsomes; HLM, human liver microsomes; HPM, human pulmonary microsomes; HRM, human renal microsomes; MJM, mouse jejunum microsomes; MLM, mouse liver microsomes; MPM, mouse pulmonary microsomes; MRM, mouse renal microsomes; RJM, rat jejunum microsomes; RLM, rat liver microsomes; RPM; rat pulmonary

microsomes; RRM, rat renal microsomes; RT-PCR, reverse transcription-polymerase chain reaction.

Abstract

Human arylacetamide deacetylase (AADAC) is a major esterase responsible for the hydrolysis of clinical drugs such as flutamide, phenacetin, and rifampicin. Thus, AADAC is considered to be a relevant enzyme in preclinical drug development, but there is little information about species differences of AADAC. This study investigated the species differences in the tissue distribution and enzyme activities of AADAC. In human, AADAC mRNA was highly expressed in liver and gastrointestinal tracts, followed by bladder. In rat and mouse, AADAC mRNA was expressed in liver at the highest level, followed by the gastrointestinal tract and kidney. The expression levels in rat tissues were approximately 7- and 10-fold lower than those in human and mouse tissues, respectively. To compare the catalytic efficiency of AADAC between three species, each recombinant AADAC was constructed and their enzyme activities were evaluated by normalizing with the expression levels of AADAC. Flutamide and phenacetin hydrolase activities were detected by the recombinant AADAC of all species. In flutamide hydrolysis, liver microsomes of all species showed similar catalytic efficiencies, despite the lower AADAC mRNA expression in rat liver. In phenacetin hydrolysis, rat liver microsomes showed approximately 4 to 6.5-fold lower activity than human and mouse liver microsomes. High rifampicin hydrolase activity was detected only by recombinant human AADAC and human liver and jejunum microsomes. Collectively, this study clarified the species differences in the tissue distribution and enzyme activities of AADAC. The results of this study facilitate our understanding of the species difference in drug hydrolysis.

Introduction

Enzymatic drug hydrolysis plays important roles in the metabolic activation and detoxification of clinically used drugs and prodrugs including ester, amide, and thioester bond. Although several esterases are known to catalyze the drug metabolism, carboxylesterase (CES) is a representative serine esterase contributing to the hydrolysis of various drugs and xenobiotics. In human, *CES1* and *CES2* families have only 2 (*CES1* and pseudogene *CES1P1*) and single genes, respectively, although the *CES1P1* gene is altered to the functional *CES1* gene in some persons (Fukami et al., 2006). Meanwhile, rat and mouse have multiple *Ces1* and *Ces2* genes (5 and 7 genes in rat, and both 8 genes in mouse, respectively) (Holmes et al., 2010). In addition, the tissue distribution and substrate specificity of CES are different between human and rodents (Sanghani et al., 2002; Satoh et al., 2002; Luan et al., 1997). Thus, studies on species differences in CES have been advanced.

Recently, we found that human arylacetamide deacetylase (AADAC), as well as CES enzymes, is involved in drug metabolism (Watanabe et al., 2009; Watanabe et al., 2010; Nakajima et al., 2011). Human AADAC is a major serine esterase expressed in liver and intestine (Probst et al., 1994). Rodents also have single *AADAC* gene, and the amino acid identities between human and rodent (rat and mouse) AADAC are not high (68.2% and 69.9%, respectively). It was reported that rat and mouse AADAC mRNA is expressed in liver and small intestine using a limited number of tissues (Trickett et al., 2001). The function and tissue distribution of rodent AADAC were poorly understood.

Human AADAC is responsible for the hydrolysis of clinically relevant drugs such as flutamide, phenacetin, and rifamycins. Flutamide is a nonsteroidal antiandrogen drug for prostate cancer. Flutamide is mainly metabolized to 2-hydroxyflutamide, a pharmacologically active metabolite, by human cytochrome P450 (CYP) 1A2, and is also hydrolyzed to 4-nitro-3-(trifluoromethyl)phenylamine (FLU-1) by AADAC (Katchen and Buxbaum, 1975;

Schulz et al., 1988; Watanabe et al., 2009). *N*-Hydroxyl FLU-1, which is a metabolite of FLU-1 by human CYP3A4, has been suggested to be associated with hepatotoxicity (Goda et al., 2006). While phenacetin had been widely used as an analgesic antipyretic, it was withdrawn from the market because of renal failure (Sicardi et al., 1991; Gago-Dominguez et al., 1999). Phenacetin is primarily metabolized to acetaminophen by CYP1A2, and is also hydrolyzed to *p*-phenetidine by human AADAC (Butler et al., 1989; Watanabe et al., 2010). *p*-Phenetidine is considered to be further metabolized to *N*-hydroxyphenetidine, the possible metabolite causing nephrotoxicity and hematotoxicity (Wirth et al., 1982; Jensen and Jollow, 1991). From these lines of evidence, it is considered that AADAC is associated with the occurrence of flutamide and phenacetin toxicities. Rifamycins such as rifampicin, rifabutin, and rifapentine have been used as antituberculosis drugs. Rifamycins have the potential to induce various drug-metabolizing enzymes, especially CYPs (Grange et al., 1994). In addition, rifampicin is suggested to be associated with hepatotoxicity by exacerbating isoniazid and/or other antituberculosis drugs-induced hepatotoxicity, or by direct toxic injury to hepatocytes (Gangadharam, 1986). However, we demonstrated that 25-deacetylrifamycins, principal metabolites of rifamycins by AADAC in human, have lower induction potency and toxicity compared with rifamycins (Nakajima et al., 2011). Thus, AADAC seems to play a role in the attenuation of induction of drug-metabolizing enzymes and toxicity by rifamycins.

In drug development, experimental animals are frequently used to predict the excretory pathway and evaluate the toxicity of drug candidates, but sometimes species differences in drug metabolizing enzymes make extrapolations to human difficult. Because AADAC is associated with the drug toxicity as described above, investigation of species differences of AADAC will contribute to the interpretation of the data of human and experimental animals. In the present study, we investigated the species differences in tissue distribution and enzyme activities of AADAC in human, rat, and mouse.

Materials and Methods

Chemicals and Reagents. Flutamide, FLU-1, phenacetin, and rifampicin were purchased from Wako Pure Chemical Industries (Osaka, Japan). *p*-Phenetidine, aprotinin, bestatin, leupeptin, and trypsin inhibitor were purchased from Sigma-Aldrich (St. Louis, MO). 25-Desacetylrifampicin (25-deacetylrifampicin) was from Toronto Research Chemicals (Toronto, Canada). Primers were commercially synthesized at Hokkaido System Sciences (Sapporo, Japan). The random hexamer and SYBR Premix Ex Taq were from Takara (Shiga, Japan). RNAiso was from Nippon Gene (Tokyo, Japan). RevaTra Ace (Mononey Murine Leukemia Virus Reverse Transcriptase RNaseH Minus) was obtained from Toyobo (Tokyo, Japan). All other chemicals used in this study were of analytical or the highest quality commercially available.

Animals. Sprague-Dawley rats (6-week old male 160 – 180 g, and female 120 – 140 g) and C57BL/6J mice (6-week old male 20 – 25 g, and female 15 – 20 g) were obtained from SLC Japan (Hamamatsu, Japan). Animals were housed in the institutional animal facility in a controlled environment (temperature 25 ± 1°C and 12-hr light/dark cycle) with access to food and water *ad libitum*. Animals were acclimatized for a week before use. Animals were maintained in accordance with the National Institutes of Health Guide for Animal Welfare of Japan, as approved by the Institutional Animal Care and Use Committee of Kanazawa University.

RNA Preparation from Rat and Mouse Tissues and Real-Time Reverse Transcription-Polymerase Chain Reaction (RT-PCR) Analyses. Total RNA samples from rat and mouse liver, kidney, stomach, jejunum (enterocytes), lung, trachea, thymus gland, adrenal gland (rat only), pancreas, heart, spleen, bladder, testis, epididymis adipose tissue

(male rat only), prostate, ovary, and uterus were freshly isolated using RNAiso. Mouse adrenal gland was too small to be excised. Real-time RT-PCR was performed for quantitative determination of AADAC mRNA using an MX3000P real-time PCR system (Agilent Technology, La Jolla, CA). The forward and reverse primers used for PCR were rAADAC-RT-F and rAADAC-RT-R primers for rat or mAADAC-RT-F and mAADAC-RT-R primers for mouse (Table 1). A 1-μl portion of the reverse transcribed mixture was added to a PCR mixture containing 10 pmol of each primer and 12.5 μl of SYBR Premix Ex Taq solution in a final volume of 25 μl. After an initial denaturation at 95˚C for 3 min, the amplification was performed by denaturation at 95˚C for 30 sec, annealing at 54˚C (rat) or 55˚C (mouse) for 20 sec, and extension at 72˚C for 20 sec for 45 cycles. The copy numbers were calculated using standard amplification curves, which were obtained using plasmids containing a full-length cDNA as a template.

Preparation of Tissue Microsomes. Human liver microsomes (HLM) (pooled, n = 50) were purchased from BD Gentest (Woburn, MA). Human jejunum microsomes (HJM, pooled, n = 10), human renal microsomes (HRM, single donor), and human pulmonary microsomes (HPM, single donor) were purchased from Tissue Transformation Technologies (Edison, NJ).

Microsomes of pooled liver, jejunum, kidney, and lung were prepared from 5 male mice and 3 male rats according to the method of Emoto et al. (2000) with slight modifications. Liver, kidney, and lung were suspended in 3 vol of ice-cold buffer A [50 mM Tris-HCl buffer (pH 7.4) containing 150 mM KCl, 20% (v/v) glycerol, 1 mM EDTA] and homogenized using a motor-driven teflon-tipped pestle. The homogenate was centrifuged at 9,000g for 15 min, and then the supernatant was centrifuged at 105,000g for 90 min. The microsomal pellets were resuspended in 3 vol of ice-cold buffer A before resedimentation at 105,000g for 60 min. The microsomal fraction was resuspended in 1 vol of ice-cold buffer B [20% (v/v) glycerol, 250 mM sucrose] and homogenized. These procedures were carried out at 4°C. Jejunum were

divided, cut longitudinally, and then washed in ice-cold 1.15% KCl by gentle swirling and mucosal cells were gently scrapped off with microspatula. The subsequent procedure was the same as for the other tissues except the buffer A included 1 mg/ml trypsin inhibitor, 10 μM leupeptin, 0.04 U/ml aprotinin, and 1 μM bestatin. The protein concentrations were determined according to the method of Bradford (1976) using γ-globulin as the standard.

Construction of Human, Rat, and Mouse Intact and Histidine (His)-tagged AADAC Expression Vectors. To compare the enzyme activities between AADACs of three species, AADAC expression vectors with the intact cDNA sequence were constructed. The bacmid DNA containing human AADAC was constructed in our previous study (Watanabe et al., 2010). In this study, the construction of expression plasmids for rat and mouse AADAC using a Bac-to-Bac Baculovirus Expression System (Invitrogen, Carlsbad, CA) was carried out according to the manufacturer's protocol. Rat and mouse AADAC cDNAs were prepared by RT-PCR technique using total RNA from liver. The forward and reverse primers were rAADAC-F and rAADAC-R primers for rat or mAADAC-F and mAADAC-R for mouse (Table 1). The PCR product was subcloned into the pFastBac1 vector.

To normalize the reactivity of human AADAC antibody against human, rat, and mouse AADAC, His-tagged AADAC expression vectors were also constructed. AADAC cDNAs with the sequences encoding His tag (5 histidines) just before stop codon were prepared using the above pFastBac1 vector containing AADAC cDNA by PCR with the following primers: pFastBac1-F and hHis-AADAC-R for human, rHis-AADAC-F and rHis-AADAC-R for rat, or mHis-AADAC-F and mHis-AADAC-R for mouse (Table 1). The PCR products were ligated into the pFastBac1 vector using appropriate restriction enzymes.

The pFastBac1 vectors described above were transformed into DH10Bac competent cells, followed by transposition of the inserts into bacmid DNA. The sequence of the AADAC cDNA was determined using a Thermo Sequenase Cy5.5 Dye Terminator Cycle Sequencing

kit (GE Healthcare, Buckinghamshire, UK) with a Long-Read Tower DNA sequencer (GE Healthcare). In this study, the nucleotide sequences of rat and mouse AADAC are referred to as BC088143.1 and NM_023383.1, respectively. Non-recombinant bacmid DNA (mock) was also prepared by the same procedures.

Expression of Human, Rat, and Mouse AADAC in Sf21 Cells. *Spodoptera frugiperda* Sf21 cells (Invitrogen) were grown in Sf-900 II SFM containing 10% fetal bovine serum at 27°C. The recombinant and mock bacmid DNAs were separately transfected into Sf21 cells with Cellfectin Reagent (Invitrogen) and the virus was harvested by collecting the cell culture medium at 72 hr posttransfection. Cells were routinely harvested 7 days after infection, washed twice with PBS, and stored at -80°C until analysis. Cell homogenates were prepared by suspending in TGE buffer [10 mM Tris-HCl buffer (pH 7.4), 20% glycerol, 1 mM EDTA (pH 7.4)] and disrupting by freeze-thawing three times according to our previous study (Watanabe et al., 2010). Then, the suspensions were homogenized with a teflon-glass homogenizer for 10 strokes.

Immunoblot Analysis. SDS-polyacrylamide gel electrophoresis and immunoblot analysis were performed according to Laemmli (1970). To examine the expression levels of His-tagged AADAC, Sf21 cell homogenates expressing His-tagged AADAC (20 μg) were separated on 10% polyacrylamide gels and electrotransferred onto polyvinylidene difluoride membrane, Immobilon-P (Millipore, Billerica, MA). The membrane was probed with monoclonal mouse anti-tetra His antibody (Qiagen, Valencia, CA) and the corresponding fluorescent dye-conjugated second antibody, and an Odyssey infrared imaging system (LI-COR Biosciences, Lincoln, NE) were used for the detection. The band intensity was quantified using ImageQuant TL Image Analysis software (GE Healthcare). The relative expression level was determined by the band intensity.

Next, the relative reactivity of monoclonal mouse anti-human AADAC antibody (Abnova, Taipei City, Taiwan) against the recombinant AADAC of each species was determined. Homogenates of Sf21 cell expressing His-tagged human, rat, and mouse AADAC (20 μg, 41.7 μg, and 7.6 μg, respectively), which show similar band intensities with anti-tetra His antibody, were loaded. The detection method was the same as described above except that monoclonal mouse anti-human AADAC antibody was used. The relative reactivity of monoclonal mouse anti-human AADAC antibody against the AADAC of each species was determined by the band intensity.

After the reactivity of the AADAC antibody was evaluated, immunoblot analysis for recombinant intact AADAC was performed. Sf21 cell homogenates expressing recombinant, intact AADAC (20 μg) were loaded and AADAC protein was detected with monoclonal mouse anti-human AADAC antibody. The band intensity was quantified and then normalized by the reactivity of the AADAC antibody. Thus, the relative expression level of recombinant intact AADAC was estimated.

These immunoblot analyses were performed in the linear range of band intensity with respect to the amount of protein.

Flutamide, Phenacetin, and Rifampicin Hydrolase Activities. The flutamide, phenacetin, and rifampicin hydrolase activities were determined using human, rat, and mouse tissue microsomes, and Sf21 cell homogenates expressing recombinant AADAC. The flutamide hydrolase activity was determined according to Watanabe et al. (2009). A typical incubation mixture (final volume of 0.2 ml) contained 100 mM potassium phosphate buffer (pH 7.4) and various enzyme sources (microsomal proteins and Sf21 cell homogenates expressing AADAC: 0.4 mg/ml). In the preliminary study, we confirmed that the rate of FLU-1 formation was linear with respect to the protein concentrations (< 0.6 mg/ml of microsomal protein and Sf21 cells homogenates expressing AADAC) and incubation time (< 45 min).

The phenacetin deacetylase (hydrolase) activity was determined according to Watanabe et al. (2010) with a slight modification. A typical incubation mixture (final volume of 0.2 ml) contained 100 mM potassium phosphate buffer (pH 7.4), and various enzyme sources (microsomal proteins and Sf21 cell homogenates expressing human AADAC: 0.4 mg/ml; rat and mouse AADAC: 0.2 mg/ml). In the preliminary study, we confirmed that the rate of formation of *p*-phenetidine was linear with respect to the protein concentrations (< 1.0 mg/ml of microsomal proteins and Sf21 cell homogenates expressing human and rat AADAC, and < 0.2 mg/ml of Sf21 cell homogenates expressing mouse AADAC) and incubation time (< 60 min for microsomal protein and Sf21 cell homogenates expressing human AADAC, and < 10 min for Sf21 cell homogenates expressing rat and mouse AADAC).

The rifampicin deacetylase (hydrolase) activity was determined according to Nakajima et al. (2011). A typical incubation mixture (final volume of 0.2 ml) contained 100 mM potassium phosphate buffer (pH 7.4) and various enzyme sources (microsomal protein and Sf21 cell homogenates expressing human, rat, and mouse AADAC: 0.5 mg/ml). In the preliminary study, we confirmed that the rate of formation of 25-deacetylrifampicin was linear with respect to the protein concentration (< 1.5 mg/ml of microsomal protein and Sf21 cell homogenates expressing AADAC) and incubation time (< 90 min).

Each reaction was performed from three independent experiments. For the kinetic analyses of flutamide, phenacetin, and rifampicin hydrolase activity, the parameters were estimated from the fitted curves using a computer program (KaleidaGraph; Synergy Software, Reading, PA) designed for nonlinear regression analysis. The kinetic equations were obtained by fitting appropriate curves with highest R^2 values.

Results

Expression of AADAC mRNA in Human, Rat, and Mouse Tissues. The expression levels of AADAC mRNA in human, rat, and mouse tissues were determined by real-time RT-PCR analysis (Fig. 1). The integrity of the extracted total RNA was verified by gel electrophoresis of 1-μg RNA on a 0.8% agarose gel, which showed sharp and clear 28S and 18S rRNA bands (data not shown). The data of human AADAC mRNA were cited from our previous study (Watanabe et al., 2009). In human, AADAC mRNA was highly expressed in liver and gastrointestinal tracts, and moderately expressed in bladder. In rat and mouse, AADAC mRNA was expressed in liver at the highest level, followed by the gastrointestinal tract (jejunum) and kidney. In most tissues, the expression levels in rat tissues were approximately 7- and 10-fold lower than those in human and mouse tissues, respectively. Approximately 1.5 to 3.0-fold higher expression of AADAC mRNA in female rat tissues was observed compared with that in male rat tissues. However, gender differences in AADAC expression level were not detected in mouse.

Expression Levels of Recombinant Human, Rat, and Mouse AADAC in Sf21 Cells. The expression levels of human, rat, and mouse AADAC in our expression systems were determined by immunoblot analysis using monoclonal mouse anti-human AADAC antibody. However, the reactivity of the antibody against each species AADAC might be different. Therefore, Sf21 cells expressing His-tagged AADAC were established. Homogenates of Sf21 cells expressing His-tagged AADAC were loaded on SDS-PAGE and were reacted with monoclonal mouse anti-tetra His antibody (Fig. 2A). The relative band intensities (human: rat: mouse = 1.00 ± 0.22: 0.48 ± 0.06: 2.64 ± 0.17) reflect the relative expression levels of His-tagged AADAC.

According to the relative expression levels of His-tagged AADAC, homogenates of

Sf21 cells expressing His-tagged human, rat, and mouse AADAC, which show similar band intensities with anti-tetra His antibody, were loaded. The membranes of His-tagged AADACs were reacted with anti-human AADAC antibody (Fig. 2B). The relative band intensities (human: rat: mouse = 1.00 ± 0.13: 0.48 ± 0.11: 0.16 ± 0.04) reflect the relative reactivity of anti-human AADAC antibody against the AADAC of each species.

Finally, intact AADAC proteins in homogenates of Sf21 cells were detected using anti-human AADAC antibody (Fig. 2C). The relative band intensities were as follows: human: rat: mouse = 1.00 ± 0.14: 1.46 ± 0.21: 1.31 ± 0.10. These values were divided by the relative reactivity of anti-human AADAC antibody against the AADAC of each species (Fig. 2B), resulting in the correct relative expression levels of recombinant intact AADAC in our expression systems. Given that the expression level of recombinant human AADAC was 1.00 unit/mg, the rat and mouse AADAC expression levels were 3.04 units/mg and 8.20 units/mg, respectively. In the subsequent study, the enzyme activities by the expression systems were normalized with these units.

Kinetic Analyses of Flutamide Hydrolase Activities by Recombinant AADACs and Tissue Microsomes of Human, Rat, and Mouse. We found that AADAC is the principal enzyme in the flutamide hydrolysis in human (Watanabe et al., 2009). The flutamide hydrolase activities by recombinant AADAC and tissue microsomes of human, rat, and mouse were analyzed (Fig. 3; Table 2). For some enzyme sources, the maximum substrate concentration (0.75 mM) was not sufficiently high to determine the *K*m values because of the limited solubility of flutamide in the incubation mixture. Therefore, the *CL*int values were calculated with the initial slope of the velocity versus the substrate concentration. In recombinant AADAC (Fig. 3A), the flutamide hydrolase activities were detected in rodents as well as human and were fitted to the Michaelis-Menten equation. The *K*m, *V*max, and *CL*int values of human AADAC were 0.6 ± 0.1 mM, 1.1 ± 0.1 nmol/min/unit, and 1.7 ± 0.0

μL/min/unit, respectively. In recombinant rat AADAC, the *K*m and *V*max values were higher than those in human AADAC, resulting in a lower *CL*int value (1.0 ± 0.0 μL/min/unit). Similarly, recombinant mouse AADAC showed the higher *K*m and *V*max values, resulting in a *CL*int value (0.9 ± 0.0 μL/min/unit) that was lower than that in human AADAC. Thus, human AADAC showed the highest catalytic efficiency for flutamide hydrolysis among the three species.

Among human tissue microsomes (Fig. 3B), high flutamide hydrolase activities were detected in jejunum and liver microsomes, reflecting the high expression of AADAC mRNA in these tissues (Fig. 1A). In HRM, the activity was detected at low flutamide concentrations (Fig. 3B and Supplemental Fig. 1). Similar to recombinant human AADAC, the kinetics in HLM were fitted to the Michaelis-Menten equation. On the other hand, the kinetics in HJM and HRM were fitted to the combined Michaelis-Menten equation/substrate inhibition equation and the substrate inhibition equation, respectively. Thus, in HJM, two *K*m and *V*max values were calculated with the Michaelis-Menten equation (4.7 ± 2.1 mM and 7.8 ± 3.0 nmol/min/mg, respectively) and substrate inhibition equation (0.2 ± 0.1 mM and 1.9 ± 0.6 nmol/min/mg, respectively) (Table 2). In rat, although the activity by recombinant rat AADAC was fitted to the Michaelis-Menten equation, that in rat tissue microsomes was fitted to the Hill equation (Fig. 3C). High activity was detected in liver microsomes with a *CL*max value of 1.4 ± 0.1 μL/min/mg. In addition, the activities were also detected in rat jejunum microsomes (RJM), rat renal microsomes (RRM), and rat pulmonary microsomes (RPM) with low *CL*max values (0.1 ± 0.0 μL/min/mg to 0.2 ± 0.0 μL/min/mg). In mouse tissue microsomes (Fig. 3D), high activity was detected in liver microsomes with a *CL*int value of 1.2 ± 0.0 μL/min/mg. The activities were also detected in mouse jejunum microsomes (MJM) and mouse renal microsomes (MRM), with *CL*int values of 0.2 ± 0.0 μL/min/mg and 0.6 ± 0.0 μL/min/mg, respectively. Similar to recombinant mouse AADAC, these activities in mouse liver microsomes (MLM), MJM, and MRM were fitted to the Michaelis-Menten

equation. Mouse pulmonary microsomes (MPM) showed quite low activity. Collectively, remarkable species differences in flutamide hydrolysis were observed in jejunum.

Kinetic Analyses of Phenacetin Hydrolase Activities by Recombinant AADACs and Tissue Microsomes of Human, Rat, and Mouse. We found that AADAC is the principal enzyme responsible for the phenacetin hydrolysis in human (Watanabe et al., 2010). The phenacetin hydrolase activities by recombinant AADAC and tissue microsomes of human, rat, and mouse were analyzed (Fig. 4; Table 3). For some enzyme sources, the maximum substrate concentration (4 mM) was not sufficiently high to determine the *K*m values because of the limited solubility of phenacetin in the incubation mixture. Therefore, the *CL*int values were calculated with the initial slope of the velocity versus the substrate concentration. In recombinant AADAC (Fig. 4A), the phenacetin hydrolase activities were detected in rodents as well as human and were fitted to the Michaelis-Menten equation. The *K*m, *V*max, and *CL*int values of human AADAC were 1.8 ± 0.1 mM, 6.4 ± 0.2 nmol/min/unit, and 3.5 ± 0.1 μL/min/unit, respectively. In recombinant rat AADAC, the *K*m and *V*max values were higher than those in human AADAC, resulting in a lower *CL*int value (2.2 ± 0.0 μL/min/unit). In contrast, recombinant mouse AADAC showed *K*m and *V*max values similar to those of human AADAC, resulting in a *CL*int value of 5.7 ± 0.3 μL/min/unit. Thus, human and mouse AADAC showed higher catalytic efficiency than rat AADAC.

In human tissue microsomes (Fig. 4B), high phenacetin hydrolase activities were detected in jejunum and liver microsomes, with *CL*int values of 4.0 ± 0.1 μL/min/mg and 1.1 ± 0.0 μL/min/mg, respectively. In rat tissue microsomes (Fig. 4C), liver microsomes showed relatively high activity, and its *CL*int value was similar to those in other tissue microsomes (0.1 ± 0.0 to 0.2 ± 0.0 μL/min/mg) (Table 3) due to the high *K*m value in liver microsomes. In mouse tissue microsomes (Fig. 4D), high activity was detected in liver microsomes with a *CL*int value of 1.3 ± 0.1 μL/min/mg, which was similar to that in HLM. The *CL*int values of

other tissues (MJM: 0.1± 0.0 μL/min/mg, MRM: 0.4 ± 0.1 μL/min/mg, MPM: 0.0 ± 0.0 μL/min/mg) were lower than that of MLM. The phenacetin hydrolase activities in human, rat, and mouse tissues appeared to be correlated with the expression levels of AADAC mRNA (Fig. 1), and were fitted to the Michaelis-Menten equation, as was the case with those by recombinant AADAC.

Kinetic Analyses of Rifampicin Hydrolase Activities by Recombinant AADACs and Tissue Microsomes of Human, Rat, and Mouse. We found that AADAC is the principal enzyme responsible for the rifampicin hydrolysis in human (Nakajima et al., 2011). The rifampicin hydrolase activities by recombinant AADAC and tissue microsomes of human, rat, and mouse were analyzed (Fig. 5; Table 4). In recombinant AADACs (Fig. 5A), human AADAC showed the rifampicin hydrolase activity, which fitted the substrate inhibition equation. The *K*m, *V*max, and *CL*int values were 0.2 ± 0.0 mM, 149.0 ± 9.0 pmol/min/unit, and 0.9 ± 0.1 μL/min/unit, respectively. In contrast, rat and mouse AADAC did not show the activity.

In human tissue microsomes (Fig. 5B), jejunum and liver microsomes showed high rifampicin hydrolase activity, which fitted the substrate inhibition equation. Although the activity in HJM seemed to be higher than that in HLM, the *CL*int values in both microsomes were similar (both tissue microsomes: 0.7 ± 0.0 μL/min/mg). The *K*m values of liver and jejunum microsomes were 0.4 ± 0.0 mM and 0.3 ± 0.0 mM, respectively, which were similar to the *K*m value of human AADAC (0.2 ± 0.0 mM). In rat and mouse tissue microsomes (Figs. 5C and D), the activities were too low to calculate the kinetic parameters (Table 4). These results suggested the species differences in the substrate specificity of AADAC.

Discussion

Our recent study found that human AADAC is responsible for the hydrolysis of clinically relevant drugs such as flutamide, phenacetin, and rifamycins (Watanabe et al., 2009; Watanabe et al., 2010; Nakajima et al., 2011). Because these drugs were reported to cause adverse drug reactions, AADAC is a pharmacologically and toxicologically relevant enzyme. In drug development, a preclinical study is conducted for the prediction of clinical efficacy, metabolic pathway, and toxicity using laboratory animals. Therefore, understanding of the species difference in drug metabolism is important to evaluate the efficacy and safety for human. However, the species differences of AADAC have not been evaluated. The amino acid identities between human and rat or mouse AADAC are not high (68.2% and 69.9%, respectively) (Fig. 6), considering that there are species differences in the catalytic efficiency and substrate specificity of AADAC. In this study, we evaluated the tissue distribution and enzyme activities of human, rat, and mouse AADAC.

At first, the tissue distribution and expression levels of AADAC in the three species were investigated (Fig. 1). In all species, AADAC mRNA was highly expressed in liver. Obvious species differences in the tissue distribution of AADAC were detected in jejunum and kidney. In contrast to human and mouse, AADAC mRNA was also expressed in rat testis. However, it was not detected in rat epididymis adipose tissue. The AADAC expression levels in rat tissues were much lower than those in human and mouse tissues. Trickett et al. (2001) predicted the transcription factors associated with the expression of AADAC by comparing the sequences in the 5'-flanking regions between the human and rodent *AADAC* genes. However, no information on the transcription factors causing different expression levels between human/mouse and rat was obtained. In addition, for rat, the AADAC expression levels in females were approximately 1.5 to 3.0-fold higher than those in males. However, a putative estrogen receptor response element was not found in the 2,000 bases of the

5'-untranslated region of rat *AADAC* genes by computer-assisted homology research. Further study on the regulatory mechanism of AADAC transcription will be necessary.

To further analyze the AADAC protein level in tissue microsomes, we performed immunoblot analysis after SDS-PAGE using liver, jejunum, pulmonary, and renal microsomes of each species (Supplemental Fig. 2A). In human, AADAC protein was expressed in liver and jejunum, but not in pulmonary and renal microsomes, which was coincident with the mRNA expression (Fig. 1). However, in rodents, the bands were detected in lung at approximately 45 kDa, which is the molecular weight of AADAC (Supplemental Fig. 2A), although the expression of AADAC mRNA was not observed in lung (Fig. 1). In addition, although rat kidney showed the lower AADAC mRNA expression and enzyme activity than liver (Fig. 1 and Fig. 3), the band intensities in rat kidney and liver were similar. To examine the possibility that the antibody can detect some proteins other than AADAC in rodents, immunoblot analysis after native PAGE was performed (Supplemental Fig. 2B). However, RRM revealed a band with the same molecular weight as recombinant AADAC and RLM. This result suggested that AADAC protein in rat kidney is moderately expressed. Considering that the enzyme activity in RRM was much lower than that in RLM, any factor(s) may be involved in the AADAC enzyme activity in rat kidney. However, the possibility that the antibody can detect some proteins other than AADAC could not be fully denied. The monoclonal mouse anti-human AADAC antibody used in this study was produced by using human AADAC partial recombinant protein with 100 amino acid residues as the immunogen, and the homologies of the corresponding region with rat and mouse AADAC were 69% and 74%, respectively. Before strict comparisons of expression levels of AADAC protein among tissues and species, we must develop specific antibodies for the various human, mouse, and rat enzymes.

Flutamide is mainly metabolized to 2-hydroxyflutamide, a pharmacologically active metabolite, by CYP1A2, and is also hydrolyzed to FLU-1 (Katchen and Buxbaum, 1975;

Schulz et al., 1988). *N*-Hydroxyl FLU-1, which is a metabolite of FLU-1 by CYP3A4, has been suggested to be associated with hepatotoxicity (Goda et al., 2006). We found that AADAC is the principal enzyme responsible for the flutamide hydrolysis in human (Watanabe et al., 2009). The present study found that rodent AADAC also catalyzed the flutamide hydrolysis (Fig 3A). The flutamide hydrolase activity in HLM followed the Michaelis-Menten equation, but those in HJM and HRM followed the substrate inhibition equation at low flutamide concentrations (Fig. 3B and Supplemental Fig. 1). Our previous study investigated the flutamide hydrolase activities in human tissue microsomes only at a high concentration (0.5 mM) (Watanabe et al., 2009). We will identify the enzyme catalyzing the flutamide hydrolysis at low concentration in the near future. The kinetics for flutamide hydrolysis by recombinant rodents AADAC and rat tissue microsomes or MPM were fitted to a different equation (Figs. 3A, C, and D). Thus, the contribution of other esterases to the flutamide hydrolysis in rodent tissues was suggested. One of the candidate esterases involved in the flutamide hydrolysis in rodents is Ces, which is responsible for the biotransformation of a number of clinical drugs. Although rodents have multiple Ces enzymes compared with human (Holmes et al., 2010), the tissue distribution and functional characterization have not been fully elucidated. Further study about their distribution and substrate specificity will be necessary to clarify the contributions of AADAC and CES to flutamide hydrolysis.

Phenacetin is primarily metabolized to acetaminophen by CYP1A2, and is also hydrolyzed to *p*-phenetidine (Butler et al., 1989). *p*-Phenetidine is thought to be further metabolized to *N*-hydroxyphenetidine, the possible metabolite causing nephrotoxicity and hematotoxicity (Wirth et al., 1982; Jensen and Jollow, 1991). Our recent study found that AADAC is the principal enzyme responsible for the phenacetin hydrolysis in human (Watanabe et al., 2010). The present study clarified that recombinant human and mouse AADAC showed higher catalytic efficiency in phenacetin hydrolysis than rat AADAC (Fig. 4; Table 3). In tissue microsomes, the *CL*int values of phenacetin hydrolysis reflected the

expression levels of AADAC mRNA (Fig. 1; Table 3). This result suggested the high contribution of AADAC to phenacetin hydrolysis in the three species. It was reported that the mutagenicity of phenacetin in *S. typhimurium* TA100 is detected only in the presence of liver S9 fractions from hamster, but not those from rat (Bartsch et al., 1980; Matsushima et al., 1980). Because the phenacetin hydrolase activity (phenacetin concentration: 1.4 mM) in hamster liver microsomes was 150-fold higher than that in RLM (Nohmi et al., 1983), it is probable that the high phenacetin hydrolase activity could induce the toxicity of phenacetin. However, there are no data about the sensitivity to phenacetin toxicity in these three species.

In flutamide and phenacetin hydrolase activities, the *K*m values in some tissue microsomes were different from those by recombinant AADAC (Tables 2 and 3). The difference of *K*m values between tissue microsomes and recombinant AADAC may be explained as follows: (1) the maximum substrate concentration was not sufficiently high to determine the *K*m values because of the limited solubilities of flutamide and phenacetin in the incubation mixture; (2) some factors expressing in tissue microsomes might alter the affinity of AADAC towards flutamide and phenacetin; (3) the activities in some tissue microsomes might be too low to calculate the appropriate *K*m values; (4) especially in flutamide hydrolysis, other enzymes would be involved in the hydrolase activity.

Rifamycins such as rifampicin and rifabutin have the potential to induce various drug-metabolizing enzymes (Grange et al., 1994). In addition, rifampicin is suggested to be associated with the hepatotoxicity (Gangadharam, 1986). Our recent study demonstrated that 25-deacetylrifamycins, the principal metabolites of rifamycins by AADAC in human, have lower induction potency and toxicity than rifamycins (Nakajima et al., 2011). Interestingly, different from human, rodent AADAC could not catalyze the rifampicin hydrolysis (Fig. 5A). Supporting this result, rifampicin hydrolase activities were detected in HLM and HJM in which AADAC was highly expressed, but were scarcely detected in rodent tissue microsomes. It was reported that 25-deacetylrifampicin is detected in human plasma as the principal

metabolite, whereas it is hardly detected in rat and rabbit plasma (Tenconi and Beretta, 1970; Chan, 1987). Binda et al. (1971) reported that dog tissues were also unable to hydrolyze rifampicin. Although we analyzed the hydrolysis of rifabutin (0.1 mM) and rifapentine (0.1 mM) that are rifamycin derivatives, their hydrolyzed metabolites were also not formed in MLM and RLM (data not shown). Thus, the 25-deacetylrifamycins might be a specific metabolite in human. The amino acid identities between human and rat or mouse AADAC are not high (68.2% and 69.9%, respectively). The differences between species in the relevant distances between sites of metabolism on substrates and the active serine residue in AADAC, the number of hydrogen bonds and π-π stacking interactions between substrates and the active site, and compound lipophilicity might partly explain the differences in the substrate recognition. Because an alternative metabolic pathway to hydrolysis in rifampicin metabolism has not been reported in rodents, it is conceivable that rifampicin is hardly metabolized in rat compared with human.

In conclusion, the present study clarified the species differences in AADAC expression tissues and enzyme activities. This is the first report that investigated AADAC species differences in drug metabolism. The substrate specificity of AADAC differs between species. The results obtained in this study will provide valuable information about species differences in drug pharmacokinetics and toxicity.

DMD Fast Forward. Published on December 29, 2011 as DOI: 10.1124/dmd.111.043067
This article has not been copyedited and formatted. The final version may differ from this version.

Acknowledgements

We acknowledge Mr. Brent Bell for reviewing the manuscript.

Authorship Contributions

Participated in research design: Yuki Kobayashi, Tatsuki Fukami, Miki Nakajima, and Tsuyoshi Yokoi

Conducted experiments: Yuki Kobayashi, Akinori Nakajima, and Akinobu Watanabe

Contributed new reagents or analytic tools: Yuki Kobayashi and Akinobu Watanabe

Performed data analysis: Yuki Kobayashi and Tatsuki Fukami

Wrote or contributed to the writing of manuscript: Yuki Kobayashi, Tatsuki Fukami, and Tsuyoshi Yokoi.

References

Bartsch H, Malaveille C, Camus AM, Martel-Planche G, Brun G, Hautefeuille A, Sabadie N, Barbin A, Kuroki T, Drevon C, Piccoli C, and Montesano R (1980) Validation and comparative studies on 180 chemicals with *S. typhimurium* strains and V79 Chinese hamster cells in the presence of various metabolizing systems. *Mutat Res* **76**: 1-50.

Binda G, Domenichini E, Gottardi A, Orlandi B, Ortelli E, Pacini B, and Fowst G (1971) Rifampicin, a general review. *Arzneimittel-Forsch* **21**: 1907-1977.

Bradford MM (1976) A rapid and sensitive method for the quantitation of microgram quantities of protein utilizing the principle of protein-dye binding. *Anal Biochem* **72**: 248-254.

Butler MA, Iwasaki M, Guengerich FP, and Kadlubar FF (1989) Human cytochrome P-450$_{PA}$ (P-450IA2), the phenacetin *O*-deethylase, is primarily responsible for the hepatic 3-demethylation of caffeine and *N*-oxidation of carcinogenic arylamines. *Proc Natl Acad Sci USA* **86**: 7696-7700.

Chan K (1987) A simultaneous determination of rifampin and 25-deacetylrifampicin in cerebrospinal fluid and plasma of rabbit by liquid chromatography. *Zhongguo Yao Li Xue Bao* **8**: 555-559.

Emoto C, Yamazaki H, Yamasaki S, Shimada N, Nakajima M, and Yokoi T (2000) Characterization of cytochrome P450 enzymes involved in drug oxidations in mouse intestinal microsomes. *Xenobiotica* **30**: 943-953.

Fukami T, Nakajima M, Maruichi T, Takahashi S, Takamiya M, Aoki Y, McLeod HL, and Yokoi T (2006) Structure and characterization of human *carboxylesterase 1A1*, *1A2*, and *1A3* genes. *Pharmacogenet Genomics* **18**: 911-920.

Gago-Dominguez M, Yuan JM, Castelao JE, Ross RK, and Yu MC (1999) Regular use of analgesics is a risk factor for renal cell carcinoma. *Br J Cancer* **81**: 542-548.

Gangadharam PR (1986) Isoniazid, rifampin, and hepatotoxicity. *Am Rev Respir Dis* **133**:

963-965.

Goda R, Nagai D, Akiyama Y, Nishikawa K, Ikemoto I, Aizawa Y, Nagata K, and Yamazoe Y (2006) Detection of new *N*-oxidized metabolite of flutamide, *N*-[4-nitro-3-(trifluoromethyl)phenyl]hydroxylamide, in human liver microsomes and urine of prostate cancer patients. *Drug Metab Dispos* **34**: 828-835.

Grange JM, Winstanley PA, and Davies PD (1994) Clinically significant drug interactions with antituberculosis agents. *Drug Saf* **11**: 242-251.

Holmes RS, Wright MW, Laulederkind SJ, Cox LA, Hosokawa M, Imai T, Ishibashi S, Lehner R, Miyazaki M, Perkins EJ, Potter PM, Redinbo MR, Robert J, Satoh T, Yamashita T, Yan B, Yokoi T, Zechner R, and Maltais LJ (2010) Recommended nomenclature for five mammalian carboxylesterase gene families: human, mouse, and rat genes and proteins. *Mamm Genome* **21**: 427-441.

Jensen CB and Jollow DJ (1991) The role of *N*-hydroxyphenetidine in phenacetin-induced hemolytic anemia. *Toxicol Appl Pharmacol* **111**: 1-12.

Katchen B and Buxbaum S (1975) Disposition of a new, nonsteroid, antiandrogen, α,α,α-trifluoro-2-methyl-4'-nitro-m-propionotoluidide (Flutamide), in men following a single oral 200 mg dose. *J Clin Endocrinol Metab* **41**: 373-379.

Laemmli UK (1970) Cleavage of structural proteins during the assembly of the head of bacteriophage T4. *Nature* **227**: 680-685.

Luan L, Sugiyama T, Takai S, Usami Y, Adachi T, Katagiri Y, and Hirano K (1997) Purification and characterization of pranlukast hydrolase from rat liver microsomes: the hydrolase is identical to carboxylesterase pI 6.2. *Biol Pharm Bull* **20**: 71-75.

Matsushima T, Yahagi T, Takamoto Y, Nagao M, and Sugimura T (1980) Species differences in microsomal activation of mutagens and carcinogens, with special reference to new potent mutagens from pyrolysates of amino acids and proteins. *Microsomes, Drug Oxidations, and Chemical Carcinogenesis*, Academic Press, New York, 1093-1102.

Nakajima A, Fukami T, Kobayashi Y, Watanabe A, Nakajima M, and Yokoi T (2011) Human arylacetamide deacetylase is responsible for deacetylation of rifamycins: rifampicin, rifabutin, and rifapentine. *Biochem Pharmacol* **82**: 1747-1756.

Nohmi T, Yoshikawa K, Nakadate M, and Ishidate M Jr (1983) Species difference in the metabolic activation of phenacetin by rat and hamster liver microsomes. *Biochem Biophys Res Commun* **110**: 746-752.

Probst MR, Beer M, Beer D, Jeno P, Meyer UA, and Gasser R (1994) Human liver arylacetamide deacetylase. Molecular cloning of a novel esterase involved in the metabolic activation of arylamine carcinogens with high sequence similarity to hormone-sensitive lipase. *J Biol Chem* **269**: 21650-21656.

Sanghani SP, Davis WI, Dumaual NG, Mahrenholz A, and Bosron WF (2002) Identification of microsomal rat liver carboxylesterases and their activity with retinyl palmitate. *Eur J Biochem* **269**: 4387-4398.

Satoh T, Taylor P, Bosron WF, Sanghani SP, Hosokawa M, and La Du BN (2002) Current progress on esterases: from molecular structure to function. *Drug Metab Dispos* **30**: 488-493.

Schulz M, Schmoldt A, Donn F, and Becker H (1988) The pharmacokinetics of flutamide and its metabolites after a single oral dose and during chronic treatment. *Eur J Clin Pharmacol* **34**: 633-636.

Sicardi SM, Martiarena JL, and Iglesias MT (1991) Mutagenic and analgesic activities of aniline derivatives. *J Pharm Sci* **80**: 761-764.

Tenconi LT and Beretta E (1970) Urinary and biliary metabolites of rifampicin in different animal species. *Proc Eur Soc Drug Toxit* **11**: 80-85.

Trickett JI, Patel DD, Knight BL, Saggerson ED, Gibbons GF, and Pease RJ (2001) Characterization of the rodent genes for arylacetamide deacetylase, a putative microsomal lipase, and evidence for transcriptional regulation. *J Biol Chem* **276**:

39522-39532.

Watanabe A, Fukami T, Nakajima M, Takamiya M, Aoki Y, and Yokoi T (2009) Human arylacetamide deacetylase is a principal enzyme in flutamide hydrolysis. *Drug Metab Dispos* **37**: 1513-1520.

Watanabe A, Fukami T, Takahashi S, Kobayashi Y, Nakagawa N, Nakajima M, and Yokoi T (2010) Arylacetamide deacetylase is a determinant enzyme for the difference in hydrolase activities of phenacetin and acetaminophen. *Drug Metab Dispos* **38**: 1532-1537.

Wirth PJ, Alewood P, Calder I and Thorgeirsson SS (1982) Mutagenicity of *N*-hydroxy-2-acetylaminofluorene and *N*-hydroxy-phenacetin and their respective deacetylated metabolites in nitroreductase deficient *Salmonella* TA98FR and TA100FR. *Carcinogenesis* **3**: 167-170.

Footnotes

This study was supported by the Japan Society for the Promotion of Science [Grant-in-Aid for Young Scientists (B) 21790148].

Send reprint requests to: Tsuyoshi Yokoi, Ph.D. Faculty of Pharmaceutical Sciences, Kanazawa University, Kakuma-machi, Kanazawa 920-1192, Japan. E-mail: tyokoi@kenroku.kanazawa-u.ac.jp

Figure legends

Fig. 1. Expression levels of AADAC mRNA in various tissues of human (A) SD rat (B) and C57BL/6J mouse (C). Copy numbers of AADAC mRNA were determined by real-time RT-PCR analyses. Each column represents the mean ± SD of triplicate determinations. ND: Not detected.

Fig. 2. (A) Representative photograph of immunoblot analysis of the expression level of His-tagged AADAC. Loaded amounts of homogenates of Sf21 cells expressing His-tagged AADAC were 20 μg. (B) Representative photograph of immunoblot analysis of the reactivity of anti-human AADAC antibody to each species AADAC. Homogenates of Sf21 cells expressing His-tagged human, rat, and mouse AADAC (20 μg, 41.7 μg, and 7.6 μg, respectively), which showed similar band intensities with anti-tetra His antibody, were loaded. (C) Representative photograph of immunoblot analysis for determination of the expression level of recombinant intact AADAC protein. Loaded amounts of homogenates expressing recombinant intact AADAC of the three species were 20 μg. These immunoblot analyses were performed in triplicate determinations.

Fig. 3. Kinetic analyses of flutamide hydrolase activities by AADAC expressed in Sf21 cells (A) and in four tissue microsomes of human (B), rat (C), and mouse (D). Total cell homogenates and microsomes were incubated with 0.025–0.75 mM flutamide (HJM were incubated with 0.005–0.75 mM flutamide). Each data point represents the mean ± SD of triplicate determinations.

Fig. 4. Kinetic analyses of phenacetin hydrolase activities by AADAC expressed in Sf21 cells (A) and in four tissue microsomes of human (B), rat (C), and mouse (D). Total cell

homogenates and microsomes were incubated with 0.05–4 mM phenacetin. Each data point represents the mean ± SD of triplicate determinations.

Fig. 5. Kinetic analyses of rifampicin hydrolase activities by AADAC expressed in Sf21 cells (A) and in four tissue microsomes of human (B), rat (C), and mouse (D). Total cell homogenates and microsomes were incubated with 0.005–1 mM rifampicin. Each data point represents the mean ± SD of triplicate determinations.

Fig. 6. Alignment of the amino acid sequence of human, rat, and mouse AADAC. Identical amino acids between three species are shown in gray boxes. The presumed active site Gly-X-Ser-X-Gly motif and aspartic acid and histidine, which complete the catalytic triad, are shown in bold type.

DMD Fast Forward. Published on December 29, 2011 as DOI: 10.1124/dmd.111.043067
This article has not been copyedited and formatted. The final version may differ from this version.

Table 1

Sequence of primers used in this study.

Primer	Sequence
For real-time RT-PCR	
rAADAC-RT-F	5'-CAGAAGGAAACATGGGAAGAAC-3'
rAADAC-RT-R	5'-CCATTTTATAGATTTTGCTACAG-3'
mAADAC-RT-F	5'-CAGAAGGAAACATGGGGAAA-3'
mAADAC-RT-R	5'-CATTTTGCAGGTTTTGTTACAG-3'
For construction of expression plasmid	
pFastBac1-F	5'-TATTCCGGATTATTCATACC-3'
hHis-AADAC-R	5'-CCCCCCGTCGACCTAGTGGTGGTGG TGGTGTAGATTTTCCTTTAGCCACT-3'
rAADAC-F	5'-GAAGATGTATATCATAGTTTACG-3'
rAADAC-R	5'-GGCTGAATTCCACAGGTACA-3'
rHis-AADAC-F	5'-CCTAGAAGAGTTGGTGTGTC-3'
rHis-AADAC-R	5'-CCCGGTACCCTAGTGGTGGTGGT GGTGCAGATTTTTGTGAAGCCAAT-3'
mAADAC-F	5'-CATCTCTGTGGTGCTTGTAG-3'
mAADAC-R	5'-ACTCATAAGTAACTGTATCGT-3'
mHis-AADAC-F	5'-GCTTAGCCCCAAAACACCAT-3'
mHis-AADAC-R	5'-CCCGGTACCTTAGTGGTGGTGGTG GTGCAGATTTTTGATAAGCCAAC-3'

h: human; r: SD rat; m: C57BL/6J mouse; F: forward primer; R: reverse primer

DMD Fast Forward. Published on December 29, 2011 as DOI: 10.1124/dmd.111.043067
This article has not been copyedited and formatted. The final version may differ from this version.

Table 2

Kinetic parameters for flutamide hydrolase activities by recombinant AADAC and tissue microsomes.

Species		*K*m or S_{50}*	*V*max	*CL*int or *CL*max†	*K*i	n
		mM	nmol/min/unit	μL/min/unit	μM	
	AADAC	0.6 ± 0.1	1.1 ± 0.1	1.7 ± 0.0	–	–
		mM	nmol/min/mg	μL/min/mg	μM	
	Liver	1.1 ± 0.0	1.9 ± 0.1	1.8 ± 0.1#	–	–
Human	Jejunum	0.2 ± 0.1[a]	1.9 ± 0.6[a]	12.9 ± 0.3#	14.0 ± 5.6[a]	–
		4.7 ± 2.1[b]	7.8 ± 3.0[b]	–	–	–
	Kidney	2.1 ± 0.1[a]	3.8 ± 0.2[a]	1.2 ± 0.0#	0.6 ± 0.1[a]	–
	Lung	ND	ND	ND	–	–
		mM	nmol/min/unit	μL/min/unit	μM	
	AADAC	5.1 ± 0.6	4.7 ± 0.5	1.0 ± 0.0#	–	–
		mM	nmol/min/mg	μL/min/mg	μM	
Rat	Liver	1.0 ± 0.0*	2.9 ± 0.3	1.4 ± 0.1†	–	1.8 ± 0.1
	Jejunum	4.2 ± 0.2*	1.7 ± 0.1	0.2 ± 0.0†	–	1.4 ± 0.1
	Kidney	5.8 ± 0.4*	2.7 ± 0.2	0.2 ± 0.0†	–	1.5 ± 0.0
	Lung	0.7 ± 0.0*	0.1 ± 0.0	0.1 ± 0.0†	–	2.1 ± 0.1
		mM	nmol/min/unit	μL/min/unit	μM	
	AADAC	3.5 ± 0.0	3.7 ± 0.1	0.9 ± 0.0#	–	–
		mM	nmol/min/mg	μL/min/mg	μM	
Mouse	Liver	7.3 ± 0.6	9.1 ± 0.6	1.2 ± 0.0#	–	–
	Jejunum	0.5 ± 0.0	0.1 ± 0.0	0.2 ± 0.0	–	–
	Kidney	0.8 ± 0.1	0.4 ± 0.0	0.6 ± 0.0#	–	–
	Lung	0.4 ± 0.0*	0.0 ± 0.0	0.0 ± 0.0†	–	5.2 ± 1.2

Data represent the mean ± SD of triplicate determinations. [a] Value calculated by the substrate inhibition equation. [b] Value calculated by the Michaelis-Menten equation. * S_{50} value calculated by the Hill equation. † *CL*max value calculated by the Hill equation. n, Hill coefficient.

*CL*int values of human AADAC and MLM were expressed as *V*max/*K*m. # If the *K*m values were relatively high, *CL*int values were calculated with initial slope of the velocity versus substrate concentration. *CL*max values were calculated with the following equation: $V\text{max} \times (n\text{-}1)/\{S_{50} \times n \times (n\text{-}1)^{1/n}\}$. ND, Not detected.

DMD Fast Forward. Published on December 29, 2011 as DOI: 10.1124/dmd.111.043067
This article has not been copyedited and formatted. The final version may differ from this version.

Table 3

Kinetic parameters of phenacetin hydrolase activities by recombinant AADAC and tissue microsomes.

Species		*K*m	*V*max	*CL*int
		mM	nmol/min/unit	μL/min/unit
	AADAC	1.8 ± 0.1	6.4 ± 0.2	3.5 ± 0.1
		mM	nmol/min/mg	μL/min/mg
Human	Liver	3.3 ± 0.2	3.6 ± 0.2	1.1 ± 0.0
	Jejunum	2.5 ± 0.1	10.0 ± 0.0	4.0 ± 0.1
	Kidney	2.3 ± 0.2	0.4 ± 0.0	0.2 ± 0.1
	Lung	7.4 ± 0.4	0.8 ± 0.0	0.4 ± 0.0#
		mM	nmol/min/unit	μL/min/unit
	AADAC	5.8 ± 0.1	12.6 ± 0.1	2.2 ± 0.0#
		mM	nmol/min/mg	μL/min/mg
Rat	Liver	29.8 ± 2.1	5.9 ± 0.4	0.2 ± 0.0#
	Jejunum	4.6 ± 0.2	0.3 ± 0.0	0.1 ± 0.0#
	Kidney	9.3 ± 0.4	0.6 ± 0.0	0.1 ± 0.0#
	Lung	5.3 ± 1.4	0.1 ± 0.0	0.1 ± 0.0#
		mM	nmol/min/unit	μL/min/unit
	AADAC	1.6 ± 0.1	9.2 ± 0.1	5.7 ± 0.3
		mM	nmol/min/mg	μL/min/mg
Mouse	Liver	9.8 ± 0.2	17.1 ± 0.4	1.3 ± 0.1#
	Jejunum	11.2 ± 2.1	1.4 ± 0.3	0.1 ± 0.0#
	Kidney	7.1 ± 0.1	2.9 ± 0.2	0.4 ± 0.1#
	Lung	2.9 ± 0.4	0.1 ± 0.0	0.0 ± 0.0

Data represent the mean ± SD of triplicate determinations. *CL*int value of human AADAC, HLM, HJM, HRM, mouse AADAC, and MPM were expressed as *V*max/*K*m. # If the *K*m value was relatively high, *CL*int value was calculated with initial slope of the velocity versus substrate concentration.

DMD Fast Forward. Published on December 29, 2011 as DOI: 10.1124/dmd.111.043067
This article has not been copyedited and formatted. The final version may differ from this version.

Table 4

Kinetic parameters for rifampicin hydrolase activities by recombinant AADAC and tissue microsomes.

Species		*K*m	*V*max	*CL*int	*K*i
		mM	pmol/min/unit	μL/min/unit	mM
	AADAC	0.2 ± 0.0	149.0 ± 9.0	0.9 ± 0.1	0.3 ± 0.1
		mM	pmol/min/mg	μL/min/mg	mM
Human	Liver	0.4 ± 0.0	272.6 ± 38.5	0.7 ± 0.0	0.2 ± 0.0
	Jejunum	0.3 ± 0.0	211.8 ± 7.4	0.7 ± 0.0	0.7 ± 0.0
	Kidney	ND	ND	ND	–
	Lung	ND	ND	ND	–
		mM	pmol/min/unit	μL/min/unit	mM
	AADAC	ND	ND	ND	–
		mM	pmol/min/mg	μL/min/mg	mM
Rat	Liver	NA	NA	0.0 ± 0.0#	–
	Jejunum	NA	NA	0.0 ± 0.0#	–
	Kidney	NA	NA	0.0 ± 0.0#	–
	Lung	NA	NA	0.0 ± 0.0#	–
		mM	pmol/min/unit	μL/min/unit	mM
	AADAC	ND	ND	ND	–
		mM	pmol/min/mg	μL/min/mg	mM
Mouse	Liver	NA	NA	0.2 ± 0.0#	–
	Jejunum	ND	ND	ND	–
	Kidney	ND	ND	ND	–
	Lung	ND	ND	ND	–

Data represent the mean ± SD of triplicate determinations. ND, Not detected. NA, Not applicable. *CL*int value of human AADAC, HLM and HJM were expressed as *V*max/*K*m. # If the *K*m value was relatively high, *CL*int value was calculated with initial slope of the velocity versus substrate concentration.

Fig. 1.

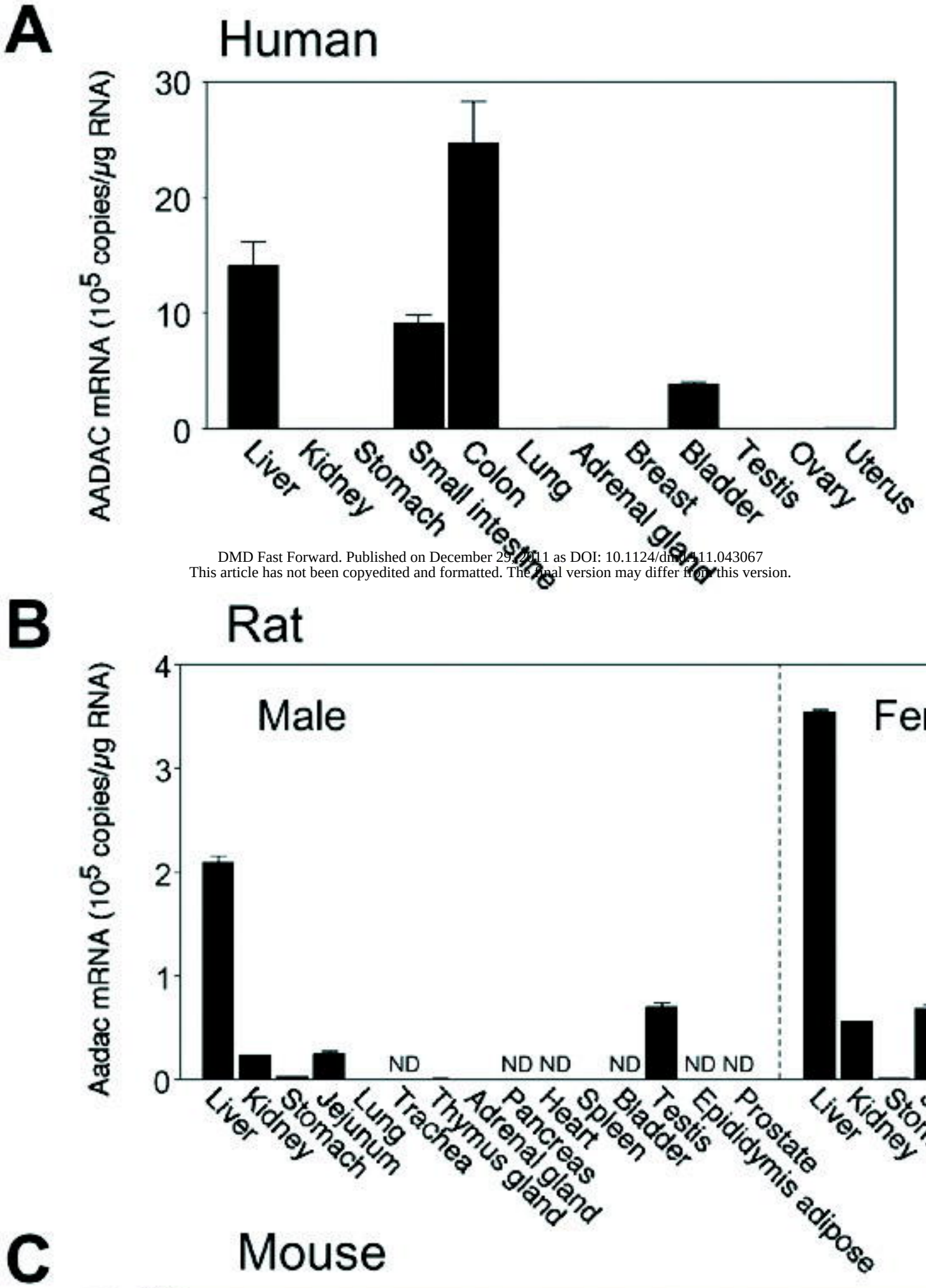

DMD Fast Forward. Published on December 29, 2011 as DOI: 10.1124/dmd.111.043067
This article has not been copyedited and formatted. The final version may differ from this version.

Fig. 2.

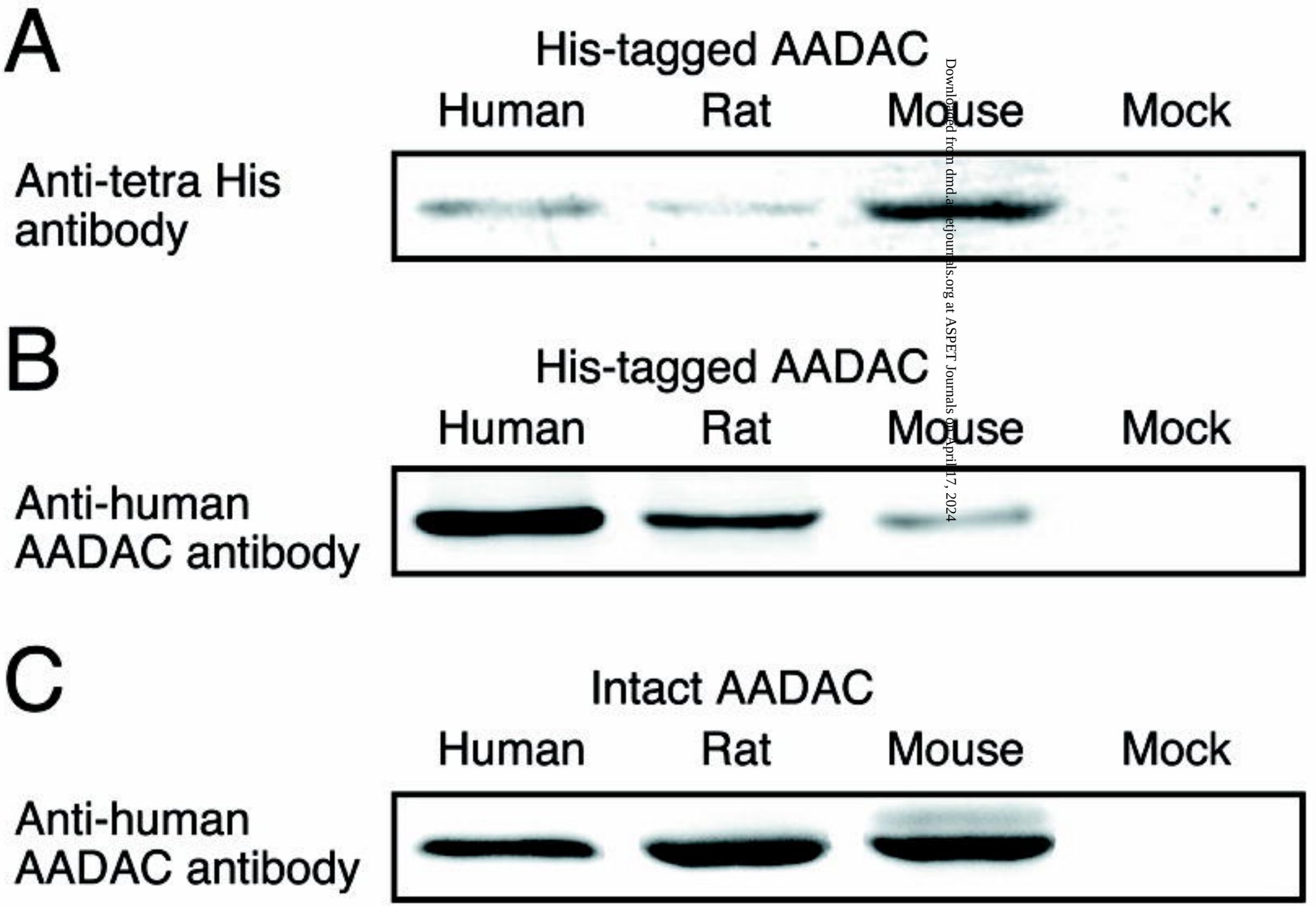

Fig. 3.

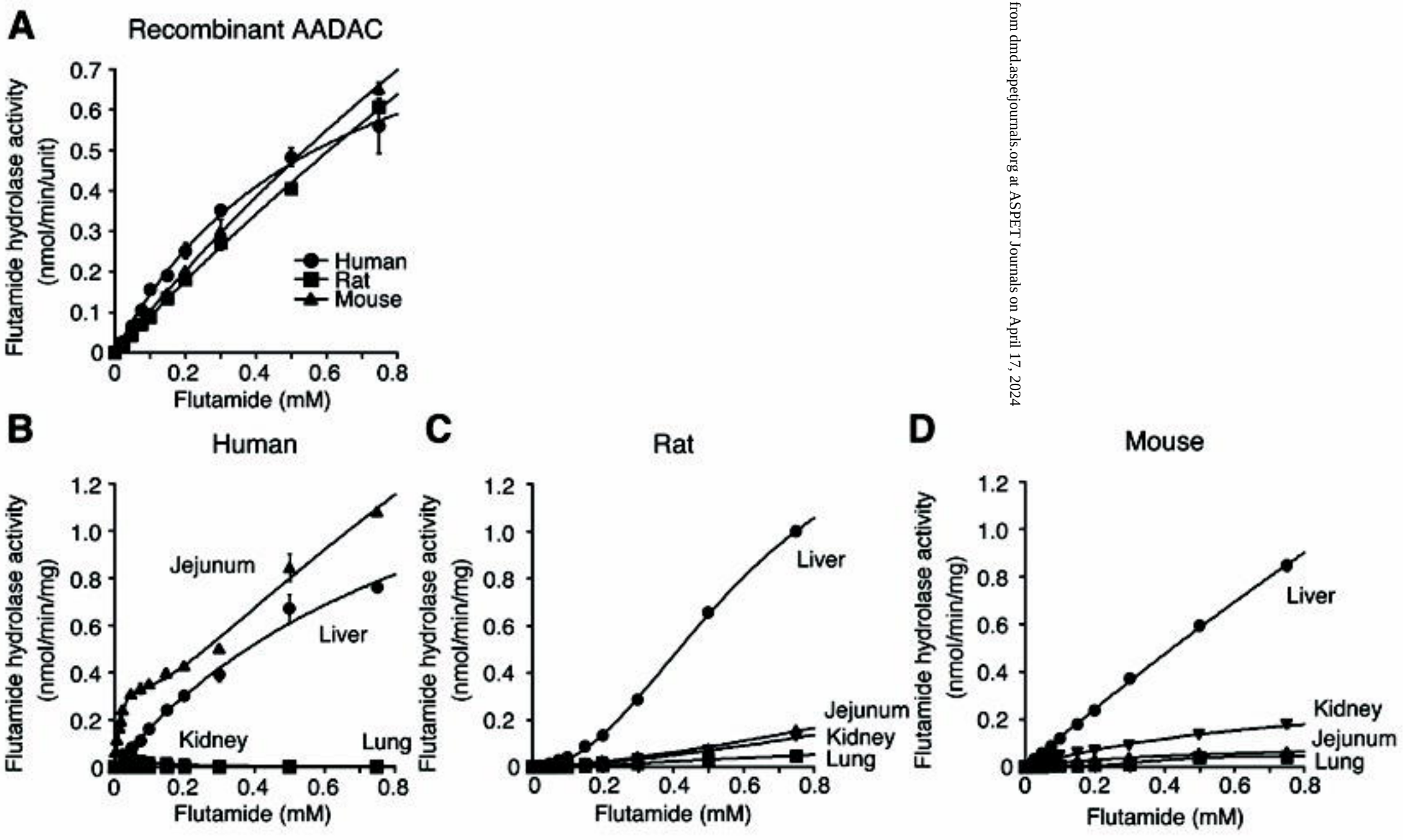

Fig. 4.

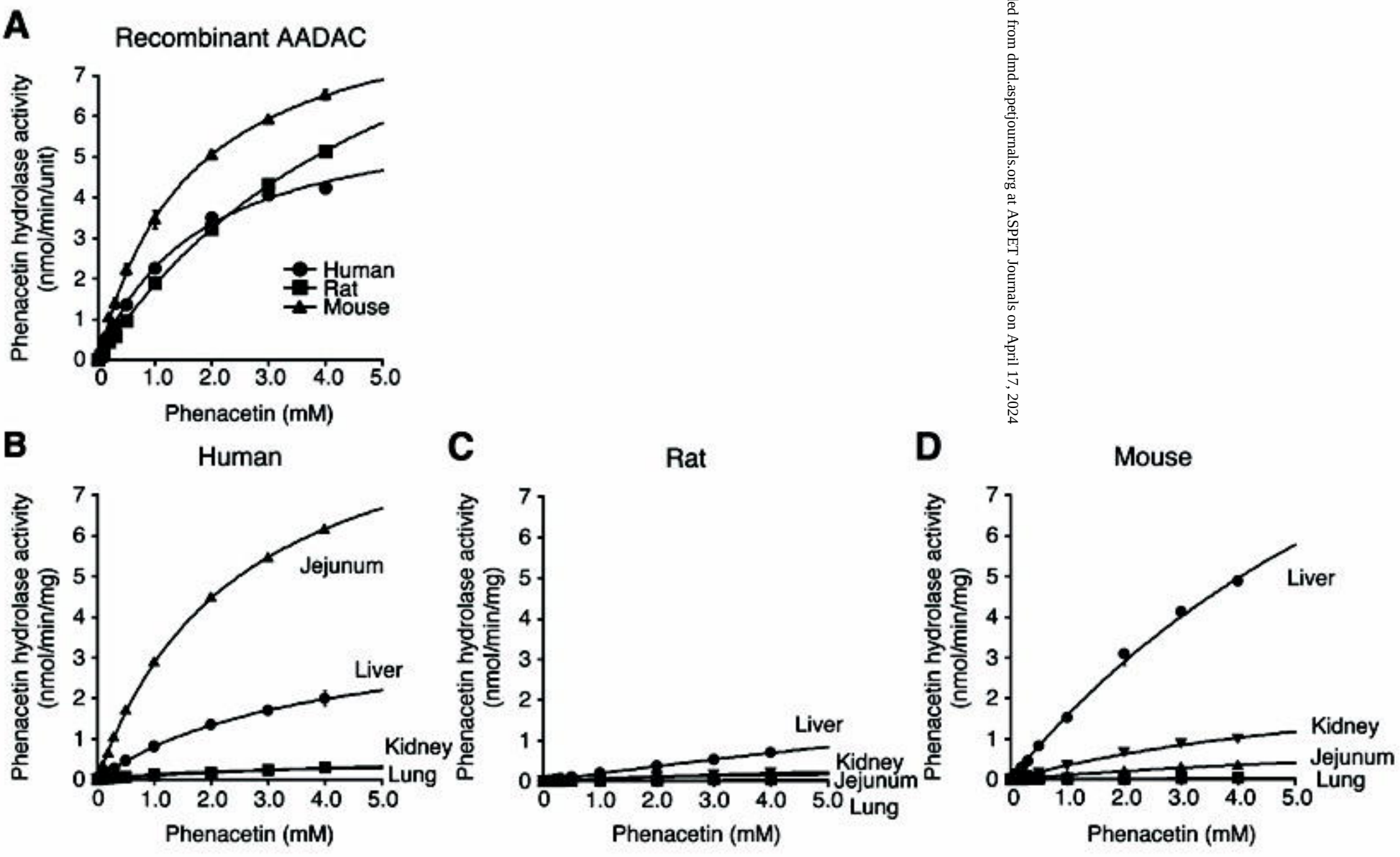

Fig. 5.

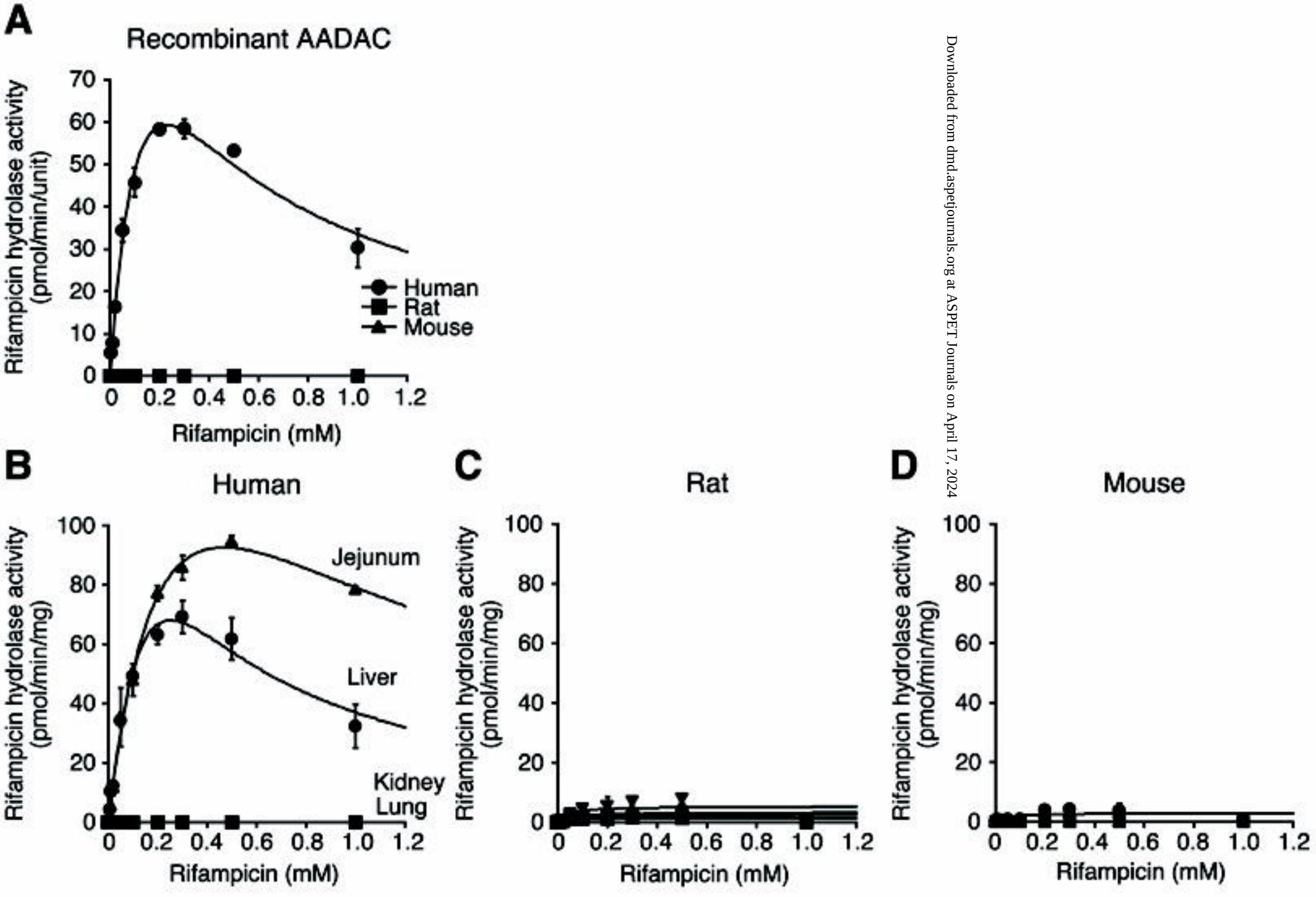

Fig. 6.


```
          1                                                              50
Human     MGRKSLYLLI VGILIAYYIY TPLPDNVEEP WRMMWINAHL KTIQNLATFV
Rat       MGRTIF-LLI SVVLVAYYIY IPLPDDIEEP WKIILGNTLL KLGGDLASFG
Mouse     MGKTIS-LLI SVVLVAYYLY IPLPDAIEEP WKVVWETAFV KIGTDLASFG

          51                                                            100
Human     ELLGLHHFMD SFKVVGSFDE VPPTSDENVT VTETKFNNIL VRVYVPKRKS
Rat       ELLGLNHFMD TVQLFMRFQV VPPTSDENVT VMETDFNSVP VRIYIPKRKS
Mouse     ELLGISHFME TIQLLMSFQE VPPTSDEHVT VMETAFDSVP VRIYIPKRKS

          101                                                           150
Human     EALRRGLFYI HGGGWCVGSA ALSGYDLLSR WTADRLDAVV VSTNYRLAPK
Rat       TTLRRGLFFI HGGGWCLGSA AYFMYDTLSR RTAHRLDAVV VSTDYGLAPK
Mouse     MALRRGLFYI HGGGWCLGSA AHFSYDTLSR WTAHKLDAVV VSTDYGLAPK

          151                                                           200
Human     YHFPIQFEDV YNALRWFLRK KVLAKYGVNP ERIGISGDSA GGNLAAAVTQ
Rat       YHFPKQFEDV YHSLRWFLQE DILEKYGVDP RRVGVSGDSA GGNLAAAVTQ
Mouse     HHFPRQFEDV YRSLRWFLQE DVLEKYGVDP RRVGVSGDSA GGNLAAAVTQ

          201                                                           250
Human     QLLDDPDVKI KLKIQSLIYP ALQPLDVDLP SYQENSNFLF LSKSLMVRFW
Rat       QILQDPDVKI KLKVQALIYP ALQALDMNVP SQQENSQYPL LTRSLLIRFW
Mouse     QLIQDPDVKI KLKVQALIYP ALQALDTNVP SQQEGSHFPV LTRSLMVRFW

          251                                                           300
Human     SEYFTTDRSL EKAMLSRQHV PVESSHLFKF VNWSSLLPER FIKGHVYNNP
Rat       SEYFTTDRDL EKAMLLNQHV PVEFSHLLQF VNWSSLLPQR YKKGYFYKTP
Mouse     SEYFTTDRGL EKAMLLNQHV PMESSHLLQF VNWSSLLPER YKKSPVYKNP

          301                                                           350
Human     NYGSSELAKK YPGFLDVRAA PLLADDNKLR GLPLTYVITC QYDLLRDDGL
Rat       TPGSLELAQK YPGFTDVKAC PLLANDSILH HLPMTYIITC QYDVLRDDGL
Mouse     TPGSSELAQK YPGFIDVKAC PLLANDNILH HLPKTYIITC QYDVLRDDGL

          351                                                           399
Human     MYVTRLRNTG VQVTHNHVED GFHGAFSFLG LKISHRLINQ YIEWLKENL
Rat       MYVKRLQNTG VHVTHHHIED GFHGALTLPG LKITYRMQNQ YLNWLHKNL
Mouse     MYVKRLQNVG VHVTHHHVED GFHGTFSFPG LKLSERMKNQ YLSWLIKNL
```